FERMILAB-CONF-16-316-E
ACCEPTED

Design and status of the Mu2e electromagnetic calorimeter

N. Atanov[a], V. Baranov[a], J. Budagov[a], R. Carosi[e], F. Cervelli[e], F. Colao[b], M. Cordelli[b], G. Corradi[b], E. Dané[b], Yu.I. Davydov[a], S. Di Falco[e], S. Donati[e,g], R. Donghia[b,j], B. Echenard[c], K. Flood[c], S. Giovannella[b], V. Glagolev[a], F. Grancagnolo[i], F. Happacher[b], D.G. Hitlin[c], M. Martini[b,d], S. Miscetti[b,*], T. Miyashita[c], L. Morescalchi[e,f], P. Murat[h], D. Pasciuto[e,g], G. Pezzullo[e,g], F. Porter[c], A. Saputi[b], I. Sarra[b], S.R. Soleti[b], F. Spinella[e], G. Tassielli[i], V. Tereshchenko[a], Z. Usubov[a], R.Y. Zhu[c]

[a] *Joint Institute for Nuclear Research, Dubna, Russia*
[b] *Laboratori Nazionali di Frascati dell'INFN, Frascati, Italy*
[c] *California Institute of Technology, Pasadena, United States*
[d] *Università "Guglielmo Marconi", Roma, Italy*
[e] *INFN Sezione di Pisa, Pisa, Italy*
[f] *Dipartimento di Fisica dell'Università di Siena, Siena, Italy*
[g] *Dipartimento di Fisica dell'Università di Pisa, Pisa, Italy*
[h] *Fermi National Laboratory, Batavia, Illinois, USA*
[i] *INFN Sezione di Lecce, Lecce, Italy*
[j] *Università degli studi Roma Tre, Roma, Italy*

Abstract

The Mu2e experiment at Fermilab aims at measuring the neutrinoless conversion of a negative muon into an electron and reach a single event sensitivity of 2.5×10^{-17} after three years of data taking. The monoenergetic electron produced in the final state, is detected by a high precision tracker and a crystal calorimeter, all embedded in a large superconducting solenoid (SD) surrounded by a cosmic ray veto system. The calorimeter is complementary to the tracker, allowing an independent trigger and powerful particle identification, while seeding the track reconstruction and contributing to remove background tracks mimicking the signal. In order to match these requirements, the calorimeter should have an energy resolution of O(5)% and a time resolution better than 500 ps at 100 MeV. The baseline solution is a calorimeter composed of two disks of BaF_2 crystals read by UV extended, solar blind, Avalanche Photodiode (APDs), which are under development from a JPL, Caltech, RMD consortium. In this paper, the calorimeter design, the R&D studies carried out so far and the status of engineering are described. A backup alternative setup consisting of a pure CsI crystal matrix read by UV extended Hamamatsu MPPC's is also presented.

Keywords: Calorimetry, scintillating crystals, avalanche photodiodes, silicon photomultipliers, lepton flavour violation
PACS: 29.40.Mc, 29.40.Vj

1. Introduction

The muon to electron conversion is an example of a Charged Lepton Flavor Violating (CLFV) process. As all CLFV processes, it is strongly suppressed in the Standard Model (SM), but many models of physics behind SM predict a branching ratio accessible at current or next-generation experiments. The conversion process is complementary to CLFV processes such as $\mu \to e\gamma$ or $\mu \to 3e$ that reach different sensitivity for different classes of models, according to the relevance of loop terms or contact terms in their general Lagrangian. The Mu2e experiment [1] at Fermilab is designed to reach a single event sensitivity of 2.5×10^{-17} in the $\mu^- + Al \to e^- Al$ process, with an improvement of four orders of magnitude over the current best experimental limit [2]. The conversion results in the production of a monoenergetic conversion electron, CE, with energy equal to the muon rest mass apart from corrections for the nuclear recoil and muon binding energy (E_{ce} = 104.97 MeV). Among the potential backgrounds, the muon *Decay-In-Orbit* (or DIO) is of particular concern, since this process, $\mu^- Al \to e^- Al \nu_\mu \overline{\nu}_e$, can produce an outgoing electron that can mimic the signal in the limit that the neutrinos have zero energy.

2. The Mu2e electromagnetic calorimeter

A redundant, high-precision apparatus, inside a large solenoid (DS), covered by a highly efficient cosmic ray veto system, is required to identify conversion electrons and to reduce background sources to negligible level. A tracking system, made of low mass straw tubes, provides the high resolution spectrometer necessary to separate signal from background. The tracker is followed by a calorimeter system characterized by (i) a large acceptance for CE's (ii) a powerful μ/e particle identification (PID), (iii) an improvement of the tracking pattern recognition, (iv) a tracking independent trigger system and (v) an improved capability to remove background tracks mimicking the signal. An extended description of the calorimeter requirements can be found in Ref. [1]. In the following, the latest improvements on the calorimeter based algorithm for

*Corresponding author
Email address: Stefano.Miscetti@lnf.infn.it (S. Miscetti)

Operated by Fermi Research Alliance, LLC under Contract No. DE-AC02-07CH11359 with the United States Department of Energy.

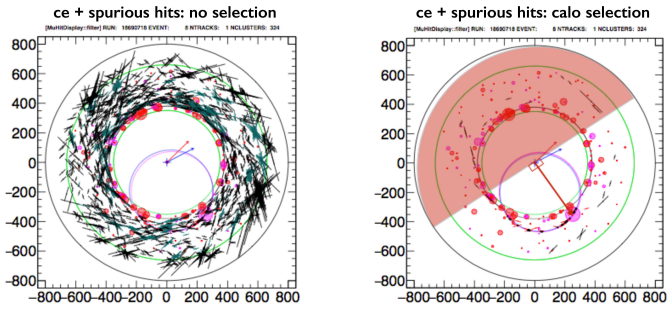

Figure 1: Example of a full simulated CE event in overlap with all hits from the environmental background: (left) without any requirement on the calorimeter system and (right) with a calorimeter based selection. Black points are hits from the tracker. Red points are from calorimeter clusters.

seeding of tracks are described. In Fig. 1, the distribution of hits in the Mu2e detector is shown for single simulated CE events. Most of the hits are due to background. By requiring the track hits to be in time with the most energetic cluster of the event, in a time window of ±50 ns, the quantity of background hits is strongly reduced, thus improving the relative reconstruction efficiency by ∼ 9%. Moreover, adding the calorimeter time information to the reconstruction of the track, the algorithm reduces hit ambiguities by 50 %, resulting in a reduction of a factor of 3 of the DIO background in the signal window.

Simulation studies show that, in order to meet the background rejection requirements, the calorimeter should have: (i) a timing resolution better than 500 ps , (ii) an energy resolution of $O(5\%)$ and (iii) a position reconstruction of $O(1$ cm) to allow a correct match with the electron track extrapolated to the calorimeter surface. A crystal based calorimeter is the adopted solution.

The crystal geometry has been optimized by means of a double disk setup to fulfill both the optimization of acceptance and the symmetric detection of e^- and e^+. The distance between the disks (70 cm) and crystal shape and dimension were tuned to increase acceptance. As a result, the baseline calorimeter consists of 1650 square crystals arranged in two disks having an inner radius of ∼ 35 cm to allow low momentum DIO electrons to pass through the central hole, without interacting with it. The calorimeter is located inside the DS: therefore it is requested to operate in presence of 1 T axial magnetic field and in a vacuum of 10^{-4} Torr. It should also be able to assure stable performance and efficiency in an environment where n, p and γ backgrounds, from muon capture processes and beam flash events, deliver a maximum dose of ∼120 Gy/year and a neutron fluence of up to 10^{12} n/cm^2/year in the hottest regions. The crystals intercept most of the neutron coming from the target so that the fluence is strongly suppressed in the second disk and in the rear part of the first disk, where a maximum fluence of up to 6×10^{10} n_{1MeVeq}/cm^2 has been estimated by our simulations.

The first choice of calorimeter components consisted of LYSO crystals [3], readout by two large area Hamamatsu avalanche photodiodes (APD) which granted the needed characteristics but the sudden cost increase of these crystals, in 2012-2013, dictated the search for alternative crystal candidates. As a result, BaF_2 crystal, a very fast scintillator, was chosen as our baseline, while retaining pure CsI as a further backup solution. In Fig. 2, the comparison of properties among LYSO, BaF_2 and pure CsI is shown. The BaF_2 is much faster than LYSO but has a reduced light yield and emits at much smaller wavelenghts. Its density is smaller than LYSO, but its radiation length and Moliere radius are still acceptable for Mu2e purposes. The emission spectrum of the BaF_2 is composed of a fast (1 ns) component at very short wavelength (< 250 nm), and a larger slower (600 ns) component at higher wavelengths (> 250 nm). The suppression of the "slow" component in the BaF_2 emission spectrum is specifically discussed in subsec. 2.3. The baseline dimension of each crystal is $3.07 \times 3.07 \times 20$ cm^3, for a total depth of 10 X_0, enough to contain the CE shower, considering that the CE impinges on the calorimeter surface with an average angle of ∼ 50°. The transverse dimension has been selected to optimize granularity and coupling to the photosensors while fulfilling the requirements on position resolution and sufficient photoelectron collection.

	LYSO	BaF_2	CsI
Radiation Length X_0 [cm]	1.14	2.03	1.86
Light Yield [% NaI(Tl)]	75	**4**/36	3.6
Decay Time[ns]	40	**0.9**/650	20
Photosensor	APD	**R&D APD**	SiPM
Wavelength [nm]	402	**220**/300	310

Figure 2: Main properties of the considered crystals.

A simulation of the baseline calorimeter geometry has been carried out with Geant4 in the Mu2e simulation framework, by inserting all details of shower development, pileup of background hits and most of the experimental effects such as: longitudinal response uniformity along the axis, non-linearity on response and electronic noise. Scaling down from measurements in progress with PMTs (subsec. 2.2), a light yield of 30 p.e./MeV and an equivalent noise of 300 keV per photosensor were assumed. With these inputs, the simulation provides an energy resolution at the level of 4.5% and a position resolution better than 7 mm for a CE. A signal shape simulation has not yet been completed: anyway a standalone simulation indicates that a timing resolution better than 200 ps can be achieved.

2.1. LYSO legacy

A 5×5 matrix prototype, built with $(30\times30\times200)$ cm^3 LYSO crystals and readout by means of S8664-1010 APDs from Hamamatsu, was assembled in Frascati to study the calorimeter performances. The LYSO matrix has been tested either with a tagged photon beam and an electron beam [4]. A 4% energy resolution and 160 ps timing resolution for 100 MeV incident particles were measured. These tests allowed a comparison between the measured resolution and the MC simulation, so to check the MC reliability.

2.2. Characterization of BaF_2 crystals

Light yield (LY) resolution and longitudinal response uniformity (LRU), of 26 prototype BaF_2 crystals have been measured: 20 crystals were produced by SICCAS (China), 2 from BGRI

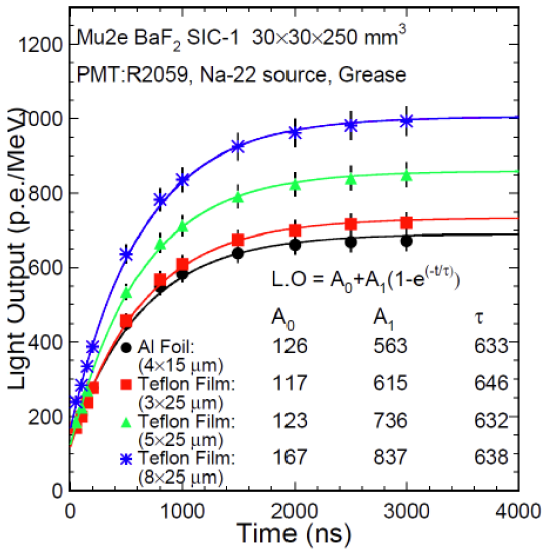

Figure 3: Light output (L.O.) of a SICCAS BaF_2 crystal as a function of the ADC integration time.

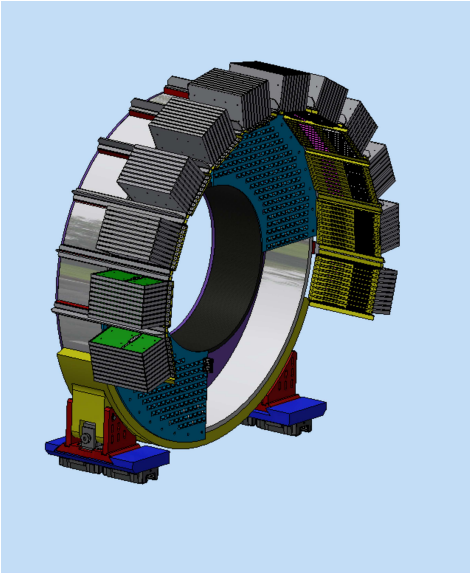

Figure 4: CAD Drawing of one of the two disks.

(China), and 2 from Incrom (Russia). The tests were carried out by illuminating crystals along the axis with a ^{22}Na source. Crystals were readout by means of a UV extended photomultiplier. One of the 511 keV annihilation photons is used as calibration source, while the second one is used as tag to clean the spectrum. In Fig. 3, the LY variation as a function of the ADC integration time is shown for SICCAS crystals: different colors corresponds to different wrapping (the highest light yield is obtained with Teflon). The dependence of the response on the integration time is well represented by a function of the form $A_0 + A_1(1 - \exp^{-t/\tau})$, where A_0, A_1 are the light yield for the fast and slow component respectively and τ is the decay time of the slow component. The longitudinal response uniformity has been studied by measuring the LY in 12 points along the axis: the distribution was fit with a linear function. The SICCAS crystals show a LY variation at both ends of ± 25% with respect to the LY in the central position, that is slightly too large for our purposes. BGRI and Incrom crystals show a smaller variation. The longitudinal transmittance of these crystals is ~ 90% at 220 nm, close to the theoretically calculated transmittance. Radiation damage tests are also in progress, both exposing crystals to a ionization dose and to a neutron fluence. For BaF_2 the damage due to the dose saturates at few hundreds Gy as reported elsewhere [5]. Light loss due to neutrons seems to be contained at few % for the fluence expected in Mu2e experiment lifetime.

2.3. *Photosensors R&D*

The slow component of BaF_2 has to be suppressed due to the high event rate in the experiment. A joint JPL/Caltech and RMD [6] consortium has been established to develop a new APD using a 9x9 mm^2 RMD device, adding a superlattice microstructure to improve the UV sensitivity and an atomic deposition layer to create an anti-reflection filter rejecting the higher wavelengths ("solar blindness"). A detailed description of the APD structure, the R&D status and of the results obtained with the first prototypes is reported in [7].

2.4. *Calorimeter Layout, FEE and readout*

The calorimeter is composed of two disks. A preliminary CAD drawing of one disk is shown in Fig. 4. The crystals will be stacked inside an external stainless steal support cylinder. An inner cylinder defines the hole where most of the low Pt particles will pass through. This inner cylinder will be made of composite material and will be connected to a front plate and to a back plate. The front face plate will be integrated with the piping transporting the Fluorine rich fluid used in the calorimeter calibration procedure (subsec. 2.5). The external support cylinder will have feet allowing to roll it over the insertion rails in the DS. In Fig. 4 the back plate for supporting photonsensors is also shown, as well as the arrangement of crates for the readout electronics. Finite element analysis has been carried out for this setup, showing negligible stress on the structure.

The electronics is composed by a FEE board directly connected to photosensor. The FEE board amplifies signals and locally regulates the bias voltages. A remote controller organized in a mezzanine board distributes bias voltages to the APDs and LV power to the preamplifiers in group of 16 channels. The amplified signals, via differential cables, reach a 16 channels board where are digitized. A sampling at 200 Msps with 12 bit resolution on a dynamic range of 2 V allows to reach the required timing performance and double pulse separation, while keeping the calorimeter data throughput inside the DAQ operation range.

2.5. *Calorimeter Calibration system*

The calorimeter calibration setup consists of: (i) a source system to equalize the crystals response and (ii) a laser system to continuously monitor the fluctuations of the APD gains. The source system is based on the BABAR scheme [8]. A Fluorine rich fluid (Fluorinert) is irradiated by neutrons from a deuterium-tritium generator, and circulated into pipes to the

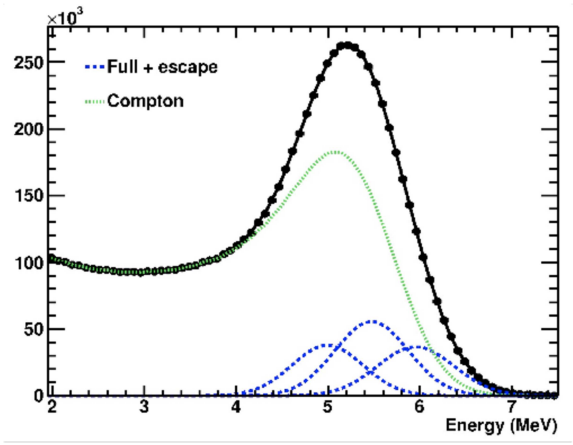

Figure 5: Simulation of source calibration run. Black points: Reconstructed energy. Thick (thin) dashed line: contribution of photon peaks (Compton).

front face of the detector. In Fig. 5, the simulated energy spectrum of the photons emitted by the excited Fluorinert is shown. It consists of a full annihilation peak at 6.13 MeV, together with single and double escape peaks at 5.62 MeV and 5.11 MeV, respectively, over the contribution of Compton photons. Even if single photon peaks cannot be separated, a clean calibration signal appears over a rather flat background. In few minutes of running, the energy scale of each crystal can be set with high precision ($< 0.5\%$). We plan to use it on regular base to follow the variation of the overall calorimeter response. Comparison with continuous laser runs will allow to disentangle the contributions of possible fluctuations due to crystal response and photosensor gain. A prototype source system is being assembled in Caltech: an operation test is expect during the summer 2015.

2.6. Backup Alternative

To test a less expensive alternative to the BaF_2 baseline, pure CsI crystals, read with the latest version of the UV extended Hamamatsu MPPC, have been studied. The characteristics of 12 pure CsI square crystals, of 3x3x20 cm^3 dimension, were measured. The crystals were produced by three different vendors. A detailed report of this study can be found in [9]. In April 2015, 10 new Silicon Protection Layer MPPC, with a quantum efficiency (at 310 nm) improved by a factor of 4 with respect to standard epoxy protected MPPC, were tested. These photosensors consist of an array of 16 3x3 mm^2 cells with 50 μm pixels, based on the new Through Silicon Vias technology allowing reduced dark rates and higher signal speed. A custom FEE board, to analogically sum all anode signals, has been developed by INFN. A fast response and good timing resolution (< 70 ps) has been observed, when the sensor is illuminated with a fast blue emitting laser light. A 3×3 CsI matrix has been built: each crystal was wrapped and was read out by one of the new photosensors optically connected to the crystal by means of Bluesil past 7 optical grease. A short test beam has been carried out at the test beam facility in Frascati National Laboratories to determine the response and resolution for 100 MeV electrons. The following preliminary results have been achieved with normal

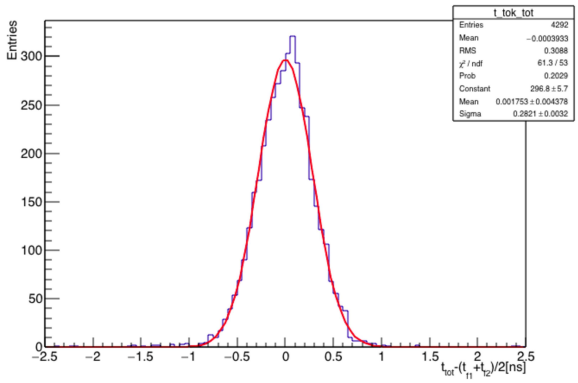

Figure 6: Distribution of the time response of the CsI(pure)+MPPC matrix prototype to 100 MeV electrons impinging at 50.° on the calorimeter surface.

incidence electrons: (i) 7 % energy resolution (ii) 250 ps timing resolution without correcting for the trigger jitter. Also data with e^- impinging at an angle of $\sim 50°$ were collected and a 280 ps timing resolution with a good Gaussian response was observed (Fig. 6). Optimization of the analysis is still under way: anyway the presented results already satisfy the calorimeter required specifications.

3. Conclusions

The Mu2e calorimeter will provide complementary information to the tracker system and will be used for PID, seeding of tracks, triggering and validating the CE track candidates. The baseline system consists of two disks of 1650 BaF_2 square crystals, each one readout by two "solar blind" APDs. Simulated performances match requirements and the test of the first APD prototypes is under way. A backup alternative, based on pure CsI crystals read by UV extended MPPC, is also under test and the preliminary results prove to match the requirements. An irradiation test of all components is under way to certify their viability in the environmental condition of the experiment. A technology review is set for summer 2015 to confirm the validity of the baseline choice and allow to complete the engineering design.

References

[1] L. Bartoszek et al. (Mu2e Experiment), "The Mu2e Technical Report", arXiv:1501.05241 (2015).
[2] W.Bertl et al., (Sindrum-II), " A search for muon to electron conversion in muonic gold", Eur. Phys. J. C47, 337 (2006).
[3] J. Budagov et al., "The calorimeter project for the Mu2e experiment", Nucl. Instrum. Meth. A 718 (2013) 56.
[4] N. Atanov et al.,"Energy and timing resolution for a LYSO matrix prototype of the Mu2e experiment", these proceedings.
[5] R.Y. Zhu et al.,"The next generation of crystal detectors", these proceedings.
[6] http://rmdinc.com/avalanche-photo-diodes/.
[7] D.G. Hitlin et al., "An APD for the detection of the fast scintillating component of BaF_2", these proceedings.
[8] B.Aubert et al., "The BABAR detector", Nucl. Instrum. Meth. A479 (2002) 1.
[9] M.Angelucci et al., "Longitudinal uniformity, time performances and irradiation test of pure CsI crystals", these proceedings.